Lu *et al. Chin. J. Mech. Eng.* (2020) 33:85
https://doi.org/10.1186/s10033-020-00513-8

Chinese Journal of Mechanical Engineering

ORIGINAL ARTICLE Open Access

Tire Dynamics Modeling Method Based on Rapid Test Method

Dang Lu[1], Lei Lu[1], Haidong Wu[1*], Wei Wang[2] and Manyi Lv[2]

Abstract

Combined with the tire dynamics theoretical model, a rapid test method to obtain tire lateral and longitudinal both steady-state and transient characteristics only based on the tire quasi-steady-state test results is proposed. For steady state data extraction, the test time of the rapid test method is half that of the conventional test method. For transient tire characteristics the rapid test method omits the traditional tire test totally. At the mean time the accuracy of the two method is much closed. The rapid test method is explained theoretically and the test process is designed. The key parameters of tire are extracted and the comparison is made between rapid test and traditional test method. The result show that the identification accuracy based on the rapid test method is almost equal to the accuracy of the conventional one. Then, the heat generated during the rapid test method and that generated during the conventional test are calculated separately. The comparison shows that the heat generated during the rapid test is much smaller than the heat generated during the conventional test process. This benefits to the reduction of tire wear and the consistency of test results. Finally, it can be concluded that the fast test method can efficiently, accurately and energy-efficiently measure the steady-state and transient characteristics of the tire.

Keywords: Tire dynamics modeling, Rapid test method, Tire steady-state and transient characteristics, Identification of tire characteristics parameters

1 Introduction

The tire is the only part of the vehicle that is in contact with the road surface. Studying the dynamic characteristics of the tire is the basis of vehicle dynamics [1]. Tire dynamics research is based on tire dynamics testing. The accuracy of the tire dynamics model depends to a large extent on the data quality of the tire modeling test. The tire modeling test is influenced by many factors, such as temperature and tire tread wear. These factors affect the quality of the test data, so the consistency of the tire state and environmental state during the test must be ensured. However, different test methods will also make the tire state consistency different.

Beauregard et al. [2] studied the linear brake test method, the steady-state test method, transient test method, the combined brake and side slip test method by using the sweeping method of the outdoor trailer. They found that the mechanical properties of the tires are quite different at different loading and speeds.

Janowski [3] studied the test method of tire driving and braking in the winter environment. The longitudinal force of the tire under different slip ratios was collected with the method loading different longitudinal slip rate by the outdoor trailer. However, due to the limitations of the test equipment and the uncontrollability of environmental factors at that time, the reliability of the data was relatively poor. Sui et al. [4] studied and developed the tire mechanical characteristic test rig. Tire cornering characteristics test and longitudinal dynamics characteristics test were carried out using this test rig with the slip angle stepped steady state test methods. Pottinger et al. [5] measured the cornering characteristics of heavy truck tire during free rolling by trailer test, at the same time, they also studied the influence of tire inflation pressure and

*Correspondence: wuhd@jlu.edu.cn
[1] State Key Laboratory of Automotive Simulation and Control, Jilin University, Changchun 130025, China
Full list of author information is available at the end of the article

tire surface properties on the mechanical properties of tires. Liu et al. [6] analyzed the test methods of the non-steady state side slip characteristics of tires, and they also designed the steering and pure lateral motion test using the tire test rig. Sommerfeld et al. [7] pointed out that tire constraints, unevenness and other factors have influence on the vertical load control accuracy of tire dynamics testing. By improving the design of the tire force and moments sensor, the influence of the above factors on the test accuracy of the tire sensor is reduced. Sui et al. [8] built a virtual tire testing platform through a finite element method. Some special tire testing which can't completed in conventional tire testing platform can be completed in the virtual tire testing platform. Tuononen et al. [9] used trailer equipment to measure the lateral stiffness on ice and snow by a new method. Li et al. [10] obtained the lateral relaxation length of the tire through the t method of the tire side angle step test. The accuracy of the model is verified by comparing the relaxation lengths obtained by the rate of stiffness method and the slip angle step method. Qiu et al. [11] studied the different measurement methods to obtain tire relaxation length at different vertical loads.

In summary, steady-state modeling in tire dynamics studies is generally based on a quasi-steady-state test method or the stepped steady state test method. The quasi-steady-state data of the tire contains not only the steady-state characteristics but also the transient characteristics. Although the quasi-steady-state characteristic of the tire is approximately equivalent to the steady-state characteristic, the test error will be inevitably introduced by directly using quasi-steady state data for steady-state modeling. Using the stepped steady state test method, the tread wear is severe before and after tire testing, and the result data consistency is poor. Tire dynamics modeling methods based on quasi-steady-state data to build tire transient model and extract steady state data are rarely reported. Therefore, the rapid test method which is based on the quasi-steady-state test data of tires to extract steady-state data and transient parameters is a key technical research work to solve the modeling of tire dynamics test.

This paper first introduces the longitudinal transient model of the tire and the method of extracting the longitudinal transient parameters from the quasi-steady state test results, and then introduces the lateral transient model without considering the turn-slip properties and the method of extracting the lateral transient parameters. Based on the above theory and method, a tire rapid quasi-steady-state test is designed, and the parameters of the transient characteristics and steady-state characteristics are extracted. Finally, the tire transient characteristics, steady-state characteristics and friction work are compared with the results obtained by the conventional tests.

2 Tire Longitudinal Transient Model

The longitudinal characteristics of the tire include longitudinal steady state characteristics and longitudinal transient characteristics. In this paper, based on the longitudinal quasi-steady-state test results, the longitudinal relaxation length which represent the transient characteristics of the tire is extracted. The transient characteristics extraction method is based on the longitudinal transient model of the tire.

2.1 Tire Longitudinal Transient Modeling

The longitudinal transient characteristics of the tire is mainly caused by the elasticity of the tire carcass, which is reflected by the hysteresis of the longitudinal force of the tire relative to the driving torque of the tire [12–16]. The parameter reflecting longitudinal transient characteristics of the tire is the longitudinal relaxation length.

The longitudinal transient model of the tire is shown in Figure 1 [14, 17, 18], where u is the longitudinal deformation of the carcass, $\dot{u}$ is the longitudinal deformation rate of the carcass, K is the longitudinal stiffness of the carcass, C is the longitudinal damping of the tread, and V_x is the longitudinal speed of the tire, V_{sx} is the longitudinal slip speed of the tire. Ω is the tire rolling rotational velocity, and R_e is the effective rolling radius of the tire.

Assuming that the longitudinal force of the tire is F_x at this time, based on the principle of force balance, Eq. (1) can be obtained:

$$\begin{cases} F_x = -C \cdot (V_x - \dot{u}) = C \cdot V_{sx}, \\ F_x = -K \cdot u. \end{cases} \tag{1}$$

Taking the derivative of second formula in Eq. (1) with respect to time:

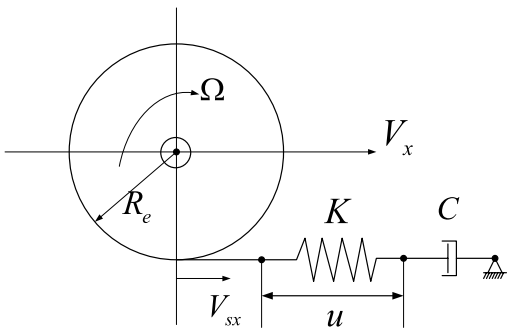

Figure 1 Schematic diagram of longitudinal transient model

$$\dot{u} = -\frac{\dot{F}_x}{K}. \tag{2}$$

In the tire dynamics model, the longitudinal force and the longitudinal slip ratio of the tire are linearly changed in a small slip state, so there is the following equation:

$$F_x = S_x \cdot K_x = -\frac{V_{sx}}{V_r} \cdot K_x = -\frac{K_x}{V_r} \cdot V_{sx}, \tag{3}$$

where S_x is the longitudinal slip ratio of the tire; K_x is the longitudinal slip stiffness of the tire; V_r is the tire rolling speed.

According to the tire steady characteristic at small slip ratio, the expression of the tread damping coefficient is:

$$C = -\frac{K_x}{V_r}. \tag{4}$$

Substituting Eq. (2) into Eq. (1), Eqs. (5) and (6) can be obtained:

$$F_x = -C \cdot (V_{sx} + \frac{\dot{F}_x}{K}), \tag{5}$$

$$-C \cdot V_{sx} = F_x + \frac{\dot{F}_x \cdot C}{K}. \tag{6}$$

Bring Eq. (4) into Eq. (6), Eq. (7) can be obtained:

$$\frac{V_{sx}}{V_r} \cdot K_x = F_x - \dot{F}_x \cdot \frac{K_x}{V_r \cdot K} = F_x - \dot{F}_x \cdot \frac{K_x}{K} \cdot V_r. \tag{7}$$

According to the definition of the longitudinal relaxation length l_x, Eq. (8) can be obtained:

$$l_x = \frac{K_x}{K}. \tag{8}$$

Bring Eq. (8) into Eq. (7), Eq. (9) can be obtained:

$$-S_x \cdot K_x = F_x - \dot{F}_x \cdot \frac{l_x}{V_r}. \tag{9}$$

When $S_x = 0$, the longitudinal relaxation length expression of the tire can be obtained by transforming Eq. (9):

$$l_{x0} = \frac{F_{x0}}{\dot{F}_{x0}} \cdot V_r, \tag{10}$$

where F_{x0} is the longitudinal force at $S_x = 0$; $\dot{F}_{x0}$ is the derivative of the longitudinal force versus time at $S_x = 0$.

The longitudinal relaxation length of the tire can be solved by Eq. (10). It is necessary to obtain the value of the longitudinal force and the derivative of the longitudinal force versus time when the longitudinal slip ratio is zero, and the rolling speed of the tire.

2.2 Key Parameters Extraction Method

When the tire is sinusoidally moved within a small longitudinal slip ratio, the relationship between the longitudinal force of the tire and the longitudinal slip ratio is approximate as shown in Figure 2. Due to the transient characteristic of the tire, the longitudinal force of the tire forms a circular curve with the slip ratio.

When $S_x = 0$. F_{x01} and F_{x02} are extracted from the above figure. And the longitudinal force with the time derivation of zero point can be obtained from these two points: $\dot{F}_{x01}$ and $\dot{F}_{x02}$ at $S_x = 0$.

$$F_{x0} = \frac{|F_{x01}| + |F_{x02}|}{2}, \tag{11}$$

$$\dot{F}_{x0} = \frac{|\dot{F}_{x01}| + |\dot{F}_{x02}|}{2}. \tag{12}$$

The longitudinal relaxation length of the tire can be solved by bringing the values obtained according to Eqs. (11) and (12) into Eq. (10).

3 Tire Lateral Transient Model without Considering the Impact of Turn-slip

Lateral dynamics properties of the tire include lateral transient characteristics and lateral steady state characteristics. In this paper, the quasi-steady-state data of the tire is obtained based on the tire slip angle sweep test, the lateral relaxation length which represent the tire lateral transient characteristic is extracted from quasi-steady-state data. The lateral transient characteristics

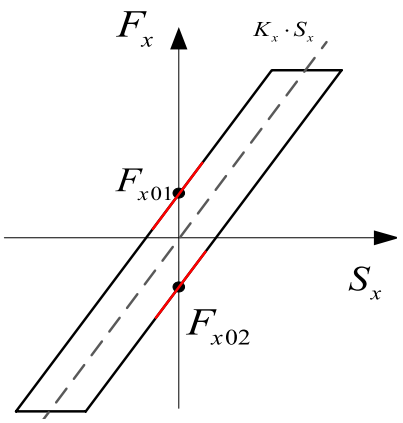

Figure 2 Schematic diagram of longitudinal transient model result

parameters are extracted based on the tire lateral transient model [16, 18, 19].

3.1 Tire Lateral Transient Model without Considering the Impact of Turn-slip

The tire lateral transient model is shown in Figure 3 [20, 21].

First, the following assumptions are proposed:

1) The carcass has only lateral translational deformation;

2) The tire only makes a small movement, and there is no slide between the tire and the road surface in the entire footprint;

3) ignore the influence of the tire width.

First the mathematical relationship between the position of the tread points and the corresponding position of the carcass in the footprint of the tire is analyzed. $P_t(X_t, Y_t)$ is the point on the tread of the tire in the footprint, and $P_c(X_c, Y_c)$ is the corresponding point on the tire carcass in the footprint. The point on the carcass and the point on the tread can be represented in global coordinates XOY. Since these points are also in the local coordinate system on the tire tread, the tread point y-axis coordinate can be expressed as $Y_t = Y_t(X, x)$. The y-axis coordinate of the point on the same carcass can also be expressed as $Y_c = Y_c(X, x)$. When the tire tread is at the front end of the grounding footprint, the point P_t on the tread and the point P_c on the carcass coincide with each other, and the following relationship exists:

$$\begin{cases} Y_t(X, a) = Y_c(X, a), \\ X_t(X, a) = X_c(X, a). \end{cases} \tag{13}$$

After entering the footprint, since the tire tread does not slip relative to the road surface, the point coordinate position on the tread can be converted to the coordinate position just entering the grounding footprint, the following expression exists:

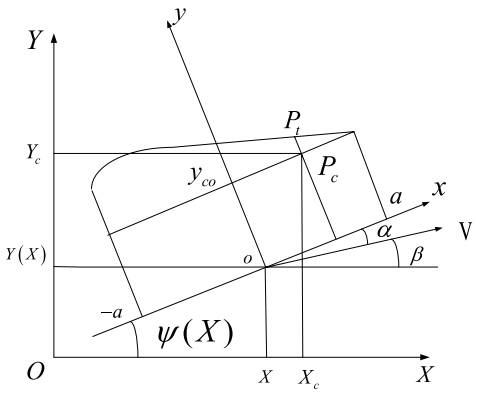

Figure 3 Schematic diagram of lateral transient modelling

$$\begin{cases} Y_t(X, x) = Y_t(X - (a - x), a), \\ X_t(X, x) = X_t(X - (a - x), a). \end{cases} \tag{14}$$

By making a difference between the ordinate of the point on the tread and the ordinate of the point on the carcass, the lateral deformation of the tread can be obtained, and the following equation is obtained:

$$\begin{cases} \Delta y(X, x) = Y_t(X, x) - Y_c(X, x), \\ \Delta y(X, x) = Y(X - (a - x)) - Y(X) + y_{c0}(X - (a - x)), \\ \quad - y_{c0}(X) + a \cdot \psi(X - (a - x)) - x \cdot \psi(X), \end{cases} \tag{15}$$

where ψ is the steering angle.

The uniform lateral force expression of the tire in the footprint is:

$$\mathrm{d}F_y = k_{ty} \Delta y \mathrm{d}x, \tag{16}$$

where k_{ty} is the bristles lateral distributed stiffness.

The expression of the lateral force of the tire in the entire grounding footprint can be obtained by combining Eqs. (15) and (16):

$$F_y(X) = k_{ty} \int_{-a}^{a} \Delta y(X, x) \mathrm{d}x. \tag{17}$$

As can be seen from the above Eq. (17), the lateral force $F_y(X)$ of the tire is a function of the distance X. According to the Laplace transform, the Laplace transformation of the lateral force $F_y(X)$ with respect to the travel distance X can be obtained as:

$$F(s) = \int_0^{+\infty} F(X) \cdot e^{-sX} \mathrm{d}X. \tag{18}$$

Bringing Eq. (17) into Eq. (18), the Laplace transform expression of the lateral force can be obtained:

$$F_y(s) = k_{ty} \int_{-a}^{a} \Delta y(s, x) \mathrm{d}x. \tag{19}$$

It is known from the static mechanical properties of the tire:

$$y_c(X) = \frac{F_y(X)}{K_{cy}} = \frac{F_y(X)}{2ak_{cy}}. \tag{20}$$

Based on Laplace transformation Eq. (21) can be obtained:

$$y_c(s) = \frac{F_y(s)}{K_{cy}} = \frac{F_y(s)}{2ak_{cy}}. \tag{21}$$

By taking a Laplace transformation on the second formula in Eq. (15), the following equation can be obtained:

$$\Delta y(s,x) = (a-x)\cdot\psi(s) - aQ(s)\cdot(1-e^{-(a-x)s}). \tag{22}$$

Among them

$$Q(s) = \psi(s) + \frac{Y(s)}{a} + \frac{y_c(s)}{a}. \tag{23}$$

A zero-order E function is defined:

$$E(s) = \frac{1}{2a}\int_{-a}^{a}(1-e^{-(a-x)s})\mathrm{d}x. \tag{24}$$

Based on Eq. (22), bring Eq. (20) into Eq. (16), Eq. (25) can be obtained.

$$F_y(s) = 2a^2k_{ty}(\psi(s) - Q(s)\cdot E(s)). \tag{25}$$

Based on Eq. (23) and Eq. (25), Eq. (26) can be obtained:

$$F_y(s) = 2a^2k_{ty} - \varepsilon_0 E(s)\cdot F_y(s), \tag{26}$$

where ε_0 (the translation feature ratio) is the ratio of tread translational distribution stiffness to carcass translational distribution stiffness, and

$$\varepsilon_0 = \frac{k_{ty}}{k_{cy}}. \tag{27}$$

Ignoring the high-order terms the one-order approximation of Taylor expansion of zero-order E function can be obtained:

$$E(s) \approx as. \tag{28}$$

According to the definition of lateral relaxation length l_y:

$$l_y = \frac{K_y}{K_{cy}} = \frac{2\cdot a^2\cdot k_{ty}}{2\cdot a\cdot k_{cy}} = a\frac{k_{ty}}{k_{cy}} = a\cdot\varepsilon_0. \tag{29}$$

The expression of the lateral force of the tire can be obtained based on Eqs. (25), (26) and (28):

$$F_y + l_y\cdot\frac{\mathrm{d}F_y}{\mathrm{d}X} = K_y\cdot\left(\psi - \frac{\mathrm{d}Y}{\mathrm{d}X} - a\cdot\frac{\mathrm{d}\psi}{\mathrm{d}X}\right). \tag{30}$$

Eq. (30) reflects the relationship between the lateral force of the tire and the lateral input in the domain of rolling distance. The relationship converted to the time domain can be obtained as follows:

$$F_y + \frac{l_y}{V_r}\dot{F}_y = K_y\left(\varphi - \frac{V_y}{V_r} - a\frac{\dot{\varphi}}{V_r}\right). \tag{31}$$

Since the influence of the turn-slip properties of the tire is neglected, Eq. (31) becomes:

$$F_y + \frac{l_y}{V_r}\dot{F}_y = K_y\cdot\left(\varphi - \frac{V_y}{V_r}\right). \tag{32}$$

When the steering angle is 0, according to the correspondence of tire kinematics, the following equation can be obtained.

$$\tan(\alpha) = \frac{V_y}{V_r}, \tag{33}$$

where α is the side slip angle.

So Eq. (29) becomes:

$$l_{y0} = -\frac{F_{y0}}{\dot{F}_{y0}}\cdot V_r. \tag{34}$$

The lateral relaxation length of the tire can be solved by Eq. (34). It is necessary to obtain the value of the lateral force and the derivative of the lateral force versus time when the steering angle is zero, and the rolling speed of the tire.

3.2 Lateral Feature Parameters Extraction Method

When the steering angle move sinusoidally in a small range, the approximate relationship between the lateral force and the steering angle of the tire is as shown in Figure 4. Due to the transient characteristic of the tire, the lateral force of the tire forms a circular curve with the steering angle.

When $S_x = 0$. F_{y01} and F_{y02} are extracted from the above figure. And the lateral force and the time derivation of zero point can be obtained from these two points: $\dot{F}_{y01}$ and $\dot{F}_{y02}$ at $S_x = 0$:

$$F_{y0} = \frac{|F_{y01}|+|F_{y02}|}{2}, \tag{35}$$

$$\dot{F}_{y0} = \frac{|\dot{F}_{y01}|+|\dot{F}_{y02}|}{2}. \tag{36}$$

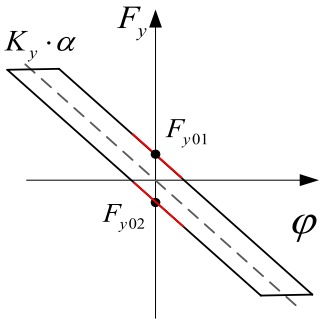

Figure 4 Schematic diagram of lateral transient model result

Figure 5 MTS CT III tire six component test rig

The lateral relaxation length of the tire can be solved by bringing the values obtained according to Eqs. (35) and (36) into Eq. (34).

4 Quasi-Steady State Rapid Test Design

The longitudinal relaxation length and the lateral relaxation length of the tire are calculated based on the extracted parameters. Due to the relative motion between the tire and the road during the test, the tire tread will inevitably wear to a certain extent. In order to reduce wear, the relative sliding distance between the tire and the road surface should be minimized. Since the speed during the test is constant, the test time should be reduced. Therefore, the steering angle loading rate of the tire should be improved during the test of the tire lateral mechanical properties. The longitudinal slip loading rate of the tire should be increased during the test of the longitudinal mechanical properties of the tire. The MTS test rig is shown in Figure 5, that is one of the best test rig with high stability and accuracy, which can minimize the effect of the test rig on the test results.

4.1 Longitudinal Rapid Test Method

According to Eq. (11), the longitudinal relaxation length of the tire is solved, and it can be obtained from the value of the longitudinal force and the derivative of the longitudinal force versus time when the longitudinal slip ratio is zero, and the rolling speed of the tire.

The tire longitudinal quasi-steady-state slip rate sweep test is carried out using a tire of the type HANKOOK 195/ 55R16. The specific test conditions are shown in Table 1.

The longitudinal quasi-steady-state slip rate sweep test result is shown in Figure 6.

Based on the test result and proposed method, the parameters characterizing the transient properties of the tire under each load are respectively obtained. The specific parameters are shown in Table 2.

Table 1 Test conditions of longitudinal quasi-steady state slip test

Vertical load (N)	Side slip angle	Camber angle	Longitudinal slip ratio	Loading ratio of longitudinal slip ratio (s^{-1})
2390	0	0	−0.3~0.3	0.1
4791	0	0	−0.3~0.3	0.1
7193	0	0	−0.3~0.3	0.1

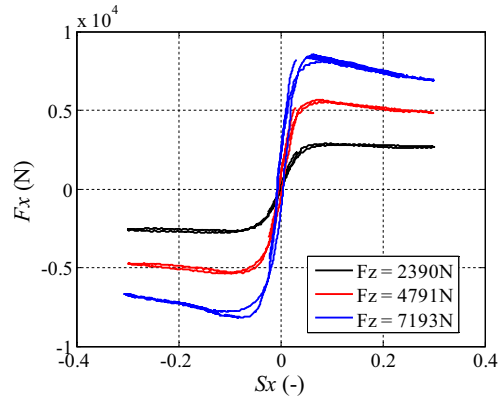

Figure 6 Result of longitudinal quasi-steady-state test

Table 2 Transient parameters of tire

Vertical load (N)	F_{x0} (N)	V_r (m/s)	$\dot{F}_x$	l_{x0} (m)
2390	144.0	16.67	9333.9	0.353
4791	724.7	16.67	21470	0.700
7193	1956.1	16.67	28233	1.111

4.2 Lateral Rapid Test Method

According to Eq. (34), the lateral relaxation length of the tire side slip is solved, and it can be obtained from the value of the lateral force and the derivative of the lateral force versus time when the steering angle is zero, and the rolling speed of the tire. In order to reduce the wear of the tire during the test, a larger steering angle loading rate is employed.

The tire lateral quasi-steady-state steering angle sweep test is carried out using a tire of the type LINGLONG 205/ 55 R16. The specific test conditions are shown in Table 3.

The results of the lateral quasi-steady-state steering angle sweep test are shown in Figure 7.

The parameters reflecting the transient characteristics of the tire are extracted from the above-mentioned steering angle sweep test results, as shown in Table 4.

Table 3 Test conditions for steering angle sweep test

Vertical load (N)	Longitudinal slip ratio	Camber angle	Steering angle (°)	Side slip angle cycle rate ((°)/s)
2041	0	0	− 16~16	4
4070	0	0	− 16~16	4
6100	0	0	− 16~16	4

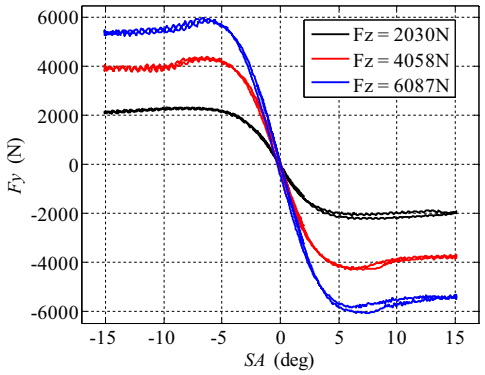

Figure 7 Result of lateral quasi-steady-state test

Table 4 Parameters for steering angle sweep test

Vertical load (N)	F_{y0} (N)	V_r (m/s)	$\dot{F}_{y0}$	l_{y0} (m)
2041	160.1	16.67	6796	0.3737
4070	452.5	16.67	11735	0.6428
6102	590.9	16.67	13732	0.7173

4.3 Steady State Data Extraction Method

According to the quasi-steady-state test data, the piecewise function fitting method is used to extract the steady-state data from the quasi-steady-state data. The specific piecewise function fitting method which is based on the steering angle sweep test data is an example. The quasi-steady-state data is divided into three parts, the first part is the linear area, and the second part is the positive side slip angle nonlinear area. The third step is the negative side slip angle nonlinear region, and the above three parts of data are extracted separately, and polynomial fitting is performed respectively, and the obtained fitting data represents the steady state data of the tire.

The tires of the type ATLAS 235 55R18 are used for the conventional steering angle sweep test and the rapid test method of steering angle sweep test. The specific test contents are shown in Table 5. The test comparison results under different loads and the comparison of the steady-state data are extracted. As shown in Figures 8, 9 and 10. The test time of the rapid test method is half that of the conventional test method.

The error calculation formula is as shown in Eq. (37):

$$dev = \frac{\sqrt{\sum \left(y_{trad} - y_{new}\right)^2}}{\sqrt{\sum \left(y_{trad}\right)^2}}, \tag{37}$$

where y_{trad} is the steady-state extraction result of conventional test method; y_{new} is the steady-state extraction result of the rapid test method.

The error calculation results under each vertical load are shown in Table 6.

It can be seen from the above results that the steady state test results extracted by the rapid test method are very close to the results extracted by the conventional test method, and the error is under 0.5%.

5 Comparison Results of Rapid Test Method and Conventional Test Method

For the longitudinal relaxation length, the stiffness ratio method is generally used to solve the problem. For the lateral relaxation length, the slip angle step method is generally used. In this paper, the relevant tests are carried out respectively, and the longitudinal relaxation length and the lateral relaxation length obtained by the conventional method and compared with the results of the rapid test method.

The friction work generated during the test of the conventional test method and the rapid test method is calculated and compared.

Table 5 Parameters for steering angle sweep test

Test methods	Vertical load (N)	Longitudinal slip ratio	Camber angle	Side slip angle (°)	Side slip angle cycle rate ((°)/s)
Conventional test method	3100 6100 9200	0	0	− 16~16	2
Rapid test method	3100 6100 9200	0	0	− 16~16	4

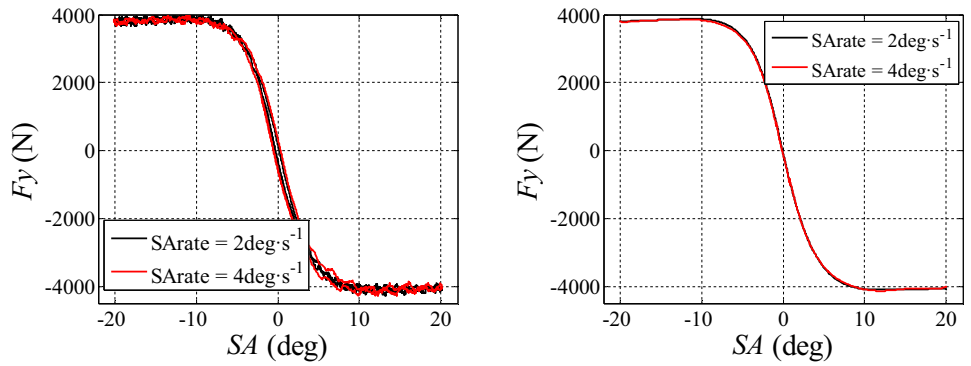

Figure 8 Lateral force test results and steady-state data extraction results under 3100 N

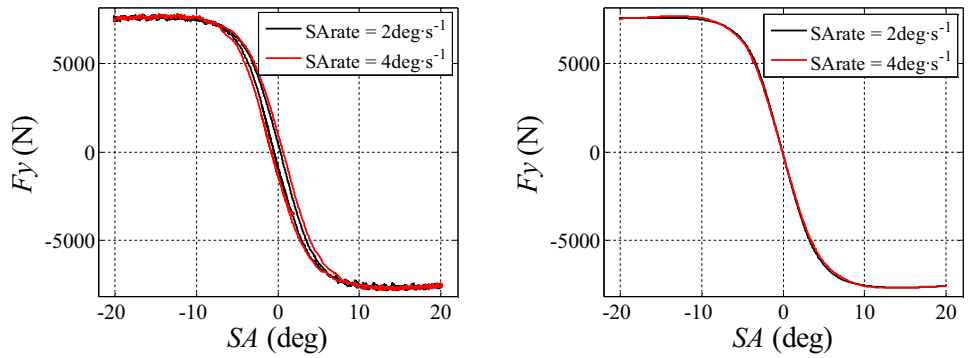

Figure 9 Lateral force test results and steady-state data extraction results under 6100 N

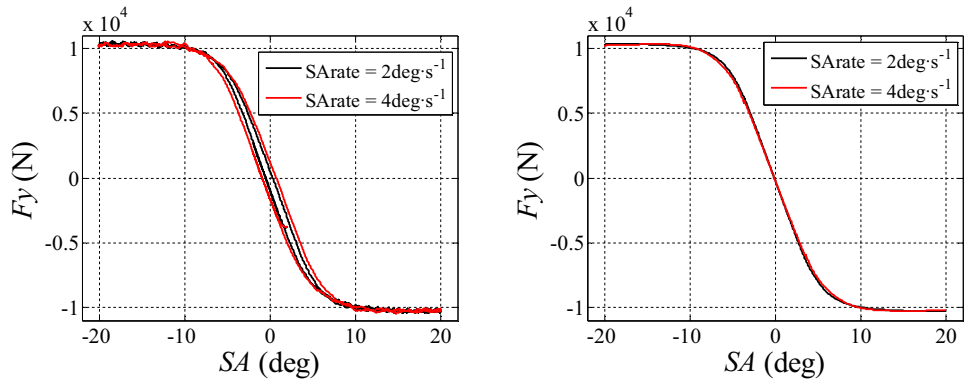

Figure 10 Lateral force test results and steady-state data extraction results under 9200 N

Table 6 Result error of rapid test method relative to conventional test method in steady state data extraction

Vertical load F_z (N)	3100	6200	9200
Error (%)	0.0318	0.073	0.126

5.1 Longitudinal Transient Test Method Comparison

The conventional longitudinal transient test method of tires is the stiffness ratio method [22, 23]. The longitudinal stiffness of the tire is obtained by the static tire longitudinal stiffness test. The longitudinal slip stiffness of the tire is obtained by the longitudinal slip steady state test.

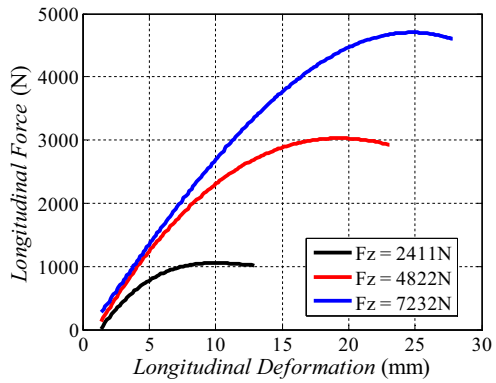

Figure 11 Result of longitudinal translational stiffness test

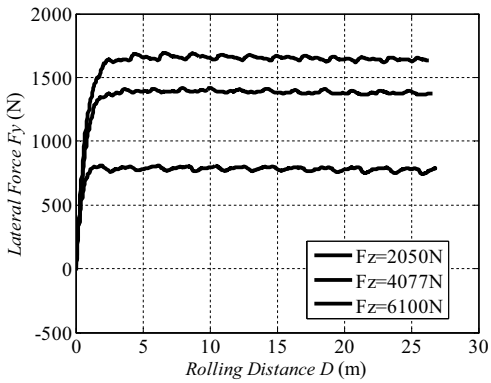

Figure 12 Result of steering angle step test

Table 7 Result of stiffness ratio method

Vertical load (N)	Longitudinal translation stiffness	Longitudinal slip stiffness	l_{xc} (m)	$\frac{l_{x0}-l_{xc}}{l_{x0}} \cdot 100\%$
2411	79541.4	144800	0.342	−3.216
4822	176749	252500	0.700	0
7232	275576	251300	1.097	−1.276

Table 8 Result of steering angle step test

Vertical load (N)	l_{yc} (m)	$\frac{l_{y0}-l_{yc}}{l_{y0}} \cdot 100\%$
2041	0.3779	1.11%
4070	0.6492	0.99%
6102	0.7282	1.49%

The static test results of the tire are shown in Figure 11, and the longitudinal translational stiffness of the tire is calculated.

Then, the tire longitudinal slip stiffness is extracted from the tire quasi-steady-state data, which is used to solve the longitudinal relaxation length of the tire. The comparison between the longitudinal relaxation length l_{xc} solved by the stiffness ratio method and l_{x0} solved by longitudinal rapid test method is shown in Table 7.

It can be seen from the above test results that error between the longitudinal relaxation length of the tire obtained by the stiffness method and the fast test method proposed in this paper are less than 4%, which meets the requirements of dynamic modeling.

5.2 Lateral Transient Test Method Comparison

The conventional tire lateral transient modeling test is based on the slip angle step test method [24–26]. The specific test method is as follows: First, the tire slip angle is set to 1° under 0 N, and then the tire load is adjusted to the test value, the data should be measured until the force is not change, the test results are shown in Figure 12.

Then, the comparison between the lateral relaxation length l_y solved by lateral rapid test method and the lateral relaxation length l_{yc} of the tire solved by side slip angle step method are shown in Table 8.

It can be seen from the above test results that the deviation between the lateral relaxation length of the tire obtained by the side slip angle step measurement method and the rapid test method proposed in this paper is less than 2%.

Table 9 Tire lateral friction work calculation comparison

Vertical load (N)	Conventional test (J)	Rapid test (J)
2041	1339.9	839.8
4070	2500.6	1588.3
6102	3475.5	2181.2

5.3 Friction Work Comparison

Tire friction work is done by the tangential force between the tire and the road surface on the tire tread [27, 28], the main energy source of the tire tread heat generation and the cause of tire tread wear.

The calculation results of friction work are shown in Table 9.

From the calculation results of the friction work under the above different loads, the friction work generated in the conventional test process is greater than that generated in the test process of the rapid test method. It can be seen that the rapid test method has less heat generation, less tread wear, higher data consistency, and reliable data quality.

6 Conclusions

This paper presents a tire rapid test theory and method for quickly and accurately obtaining tire steady-state and transient characteristics. The rapid test method obtained the transient and steady-state characteristics of the tire through a quasi-steady state test. The rapid test method proposed greatly shortens the time used for testing and improves the modeling efficiency of tire dynamics test on the basis of ensuring the quality of test data and the accuracy of the model. Moreover, the accuracy of the transient model parameters and the accuracy of the steady-state test data measured by the rapid test method are almost equal to those of the conventional modeling and test method, but the test efficiency and modeling efficiency are higher than the conventional method.

Acknowledgements
The authors sincerely thanks to Dr. Ting Xu for his critical discussion and reading during manuscript preparation.

Authors' Contributions
DL was in charge of the whole trial; LL wrote the manuscript; LL and HW made a contribution to theory and test data analyses, WW and ML assisted with sampling and laboratory analyses. All authors read and approved the final manuscript.

Funding
Supported by National Natural Science Foundation of China (Grant No. 51775224).

Competing Interests
The authors declare no competing financial interests.

Author Details
[1] State Key Laboratory of Automotive Simulation and Control, Jilin University, Changchun 130025, China. [2] General R&D Institute of China Department Experiment Unit, FAW Group Co., LTD, Changchun 130013, China.

Received: 29 November 2019 Revised: 8 November 2020 Accepted: 16 November 2020
Published online: 25 November 2020

References

[1] K H Guo, D Lu, H D Wu. Tire dynamics collaborative development strategy. *Strategic Study of CAE*, 2018, 20(1): 91–96. (in Chinese)
[2] C Beauregard, R G McNall. Tire cornering /traction test methods. *Society of Automotive Engineers*, 1973, 26(3): 136–140.
[3] William R Janowski. *Tire traction testing in the winter environment*. SAE Paper, 1980: 800–839.
[4] Jun Sui, K H Guo, W R Wei, et al. The development and debugging of a new testing bench of static properties and its application. *Journal of Jilin University of Technology*, 1995, 25(4): 1–8. (in Chinese)
[5] M G Pottinger, W Pelz. A free-rolling cornering test for heavy-duty truck tires. *Tire Science and Technology*, 1996, 24(02): 153–180.
[6] Q Liu, K H Guo. Analysis and testing of non-steady state tire cornering properties. *Journal of Jilin University of Technology*, 1998, 28(1): 2–7. (in Chinese)
[7] J L Sommerfeld, R A Meyer. *Correlation and accuracy of a wheel force transducer as developed and tested on a Flat-Trac® Tire Test System*. SAE Paper, 1999: 1999-01-0938.
[8] J Sui, J Hirshey. *Evaluation on analytical tire models for vehicle vertical vibration simulation using virtual tire testing method*. SAE Paper, 1999: 1999-01-0786.
[9] A Tuononen, T Lehtonen. Estimation of tire cornering stiffness from vehicle measurements. *Society of Automotive Engineers of Japan*, 2006: 2006-05-0479.
[10] F Li, Q W Jiang, Y Li. Study on the measurement method of tire side slip non-steady characteristic. *Journal of Chongqing University of Technology (Natural Science)*, 2018, 32(9): 29–34. (in Chinese)
[11] C F Qiu, L Zhou, J J Liu, et al. Study on test method of tire side deviation relaxation length. *Tire Industry*, 2019, 39(10): 633–636. (in Chinese)
[12] A Pandey, A Shaju. Modelling transient response using PAC 2002-based tyre model. *Vehicle System Dynamics*, 2020: 1802048.
[13] R Rugsaj, C Suvanjumrat. Development of a transient dynamic finite clement model for the drum testing of a non-pneumatic tire. *IOP Conference Series Materials Science and Engineering*, 2020, 886: 012056.
[14] H B Pacejka. *Tire and vehicle dynamics III*. Netherlands: Elsevier, 2012.
[15] M S Arslan, M Sever. Vehicle stability enhancement and rollover prevention by a nonlinear predictive control method. *Trans. Inst. Meas. Control*, 2019, 41(8): 2135–2149.
[16] V Vantsevich, L I Demkiv, S R Klos. Analysis of tire relaxation constants for modeling vehicle traction performance and handling. *ASME 2018 Dyn. Syst. Control Conf. DSCC*, 2018, 1: 113.
[17] K H Guo, Q Liu. Modelling and simulation of non-steady state cornering properties and identification of structure parameters of tyres. *Vehicle System Dynamics*, 1997, 27(S1): 80–93
[18] H B Pacejka, I J M Besselink. Magic formula tyre model with transient properties. *Vehicle System Dynamics*, 1997, 27(S1): 234–249.
[19] Y Q Zhao, Y J Deng, F Lin, et al. Transient dynamic characteristics of a non-pneumatic mechanical elastic wheel rolling over a ditch. *International Journal of Automotive Technology*, 2018, 19(3): 499–508.
[20] Q Liu, K H Guo. *Simulation of tire cornering properties in non- steady state conditions*. SAE Paper, 1998: 980254.
[21] K H Guo, D Lu, S K Chen, et al. The UniTire model: a nonlinear and non-steady-state tyre model for vehicle dynamics simulation. *Vehicle System Dynamics,* 2005, 43(Suppl.):341–358.
[22] H Yamashita, P Jayakumar, H Sugiyama. Physics-based flexible tire model integrated with LuGre tire friction for transient braking and cornering analysis. *Journal of Computational & Nonlinear Dynamics*, 2016, 11(3): 031017.
[23] V Timo, L Robert, M Martin, et al. A modular race tire model concerning thermal and transient behavior using a simple contact patch description. *Tire Science and Technology*, 2013, 41(4): 8657–8666.
[24] H Yamashita, Y Matsutani, H Sugiyama. Longitudinal tire dynamics model for transient braking analysis: ANCF-LuGre tire model. *Journal of Computational and Nonlinear Dynamics*, 2015, 10(3): 031003.
[25] C F W, O A Olatunbosun. Transient dynamic behaviour of finite element tire traversing obstacles with different heights. *Journal of Terramechanics*, 2014, 56: 1–16.
[26] H P Willumeit, F BOHM. Wheel vibrations and transient tire forces. *Vehicle System Dynamics*, 2010, 24(6-7): 525–550.
[27] S Bibin Pandey, Ashok Kumar. A hybrid approach to model the temperature effect in tire forces and moments. *SAE Journal of Passenger Cars-Mechanical System*, 2017, 10(1): 2017-01-9676.
[28] K B Singh. Estimation of tire–road friction coefficient and its application in chassis control systems. *Systems Science & Control Engineering*, 2015, 3(1): 39–61.